

**Republic of Iraq
Ministry of Higher Education
and Scientific Research
University of Babylon
College of Science for Women
Department of Chemistry**



**Synthesis ,characterization of Co_3O_4 and NiO metal oxide
nanoparticles using metal Schiff base complexes as precursor**

A project

**Submitted to the Council of the College of Science for Women,
University of Babylon in Partial Fulfilment of the Requirements for the
Degree of Bachelor's of Science in chemistry**

By

Ayat Rheem Kazar

Supervised By

Asst. Prof . Dr. Ali Taleb Bader

2023 A.D

1444 A.H

Abstract :

In this study, NiO and Co₃O₄ NPs have been efficiently synthesized by a thermal decomposition of Schiff base-M(II) complexes (M= Ni, and Co), as the promising precursors. A Schiff base ligand 2-(((5-chloropyridin-2-yl)imino)methyl)phenol was prepared through condensation reaction 2-Amino-5-chloropyridine and 2-hydroxybenzaldehyde in 1:1 molar ratio and characterized by UV-Vis, FT-IR spectroscopy, ¹H NMR, and ¹³C NMR. The synthesized Schiff-bases act as deprotonated tridentate for the complexation reaction with Co(II), and Ni(II) ions in molar ratio 1:1 and characterized by physical, spectral and analytical. The new compounds, possessing the general formula [M(L)_nH₂O]_nCH₃COOH where [M=Co(II) and Ni(II)] show an octahedral geometry. The synthesized Ni (II) and Co(II) complexes were used as precursors for Co₃O₄ and NiO nanoparticles which were characterized using XRD, FT-IR and UV-Vis spectroscopy. The crystalline structures and morphology of final products were studied by X-ray powder diffraction. By using Scherrer equation, the average crystallite size calculated for Co₃O₄ and NiO nanoparticles are 23.8 and 22.9 respectively.

Key word : Schiff Base, Metal ion complexes, Co₃O₄ and NiO nanoparticles

Introduction:

The Schiff bases are condensation products of primary amines and carbonyl compounds and they were discovered by a German chemist, the Nobel Prize winner, Hugo Schiff in 1864[1]. Schiff base have been most widely used versatile ligands, in their neutral or deprotonated forms to form stable complexes with most of the transition metal ions and still play an important role in metal coordination chemistry even after almost a century since their discovery. This class of compounds has been explored as models for biological systems[2] Due to their remarkable characteristics and applications, transition metal Schiff base complexes have recently received considerable interest[3] Sustainable visible light photocatalytic scavenging of the noxious organic pollutant using recyclable and reusable polyaniline coupled WO_3/WS_2 nanohybrid[4, 5]. In addition, Schiff base complexes are suitable choices for the preparation of nanoparticle metaloxides[6-8], which have unique chemical, optical and magnetic properties[9, 10] Among these nanosized metal oxides, Co_3O_4 , NiO, and ZnO continue to be relevant because of their numerous uses as electrode materials for supercapacitors, as an effective anode in Li-ion batteries, as glycerol electrooxidation in alkaline medium, as an efficient degrader of roxarson, as a concurrent in-situ adsorbent of secondary inorganic arsenic, photocatalytic degradation of dyes from aqueous solutions and as an extremely sensitive and specific acetone sensor[11-13].

Experimental

Materials:

The chemical compound used high purity without purification, Salicylaldehyde (Merck, Germany), 2-Amino-5-chloropyridine (Merck), Nickel acetate tetrahydrate $\text{Ni}(\text{CH}_3\text{COOH})_2 \cdot 4\text{H}_2\text{O}$ and cobalt acetate tetrahydrate $\text{Co}(\text{CH}_3\text{COOH})_2 \cdot 4\text{H}_2\text{O}$ (BDH, England).

Instrumental

In Stuart melting point (digital) SMP30 apparatus was used to record the melting point. FTIR spectra were measured by a Shimadzu (FTIR) model Broker Spectrophotometer between the ranges (4000–400) cm^{-1} as KBr discs. UV-Vis ultraviolet Spectrophotometer model 1700 Shimadzu is used to measure the UV-visible spectra at R.T. °C using 1 cm quartz cell and examined between 200–800 nm at 10^{-3} M in DMF. The ^1H - and ^{13}C -NMR spectrum of ligand was recorded at a Bruker DMX-400 spectrophotometers (400 MHz) by using DMSO-d_6 .

Procedures

Synthesized Schiff base (Ligand):

The route of synthesis of the Schiff base ligand is shown in Scheme 1 by condensation 2-Amino-5-chloropyridine (5.26 gm, 0.04 mole) with 2-hydroxy benzaldehyde (5 mL, 0.04 mol) were mixed in 20 ml of absolute ethanol with the addition of few drops of acetic acid as catalyst. The mixture was refluxed for 5 h at 70 °C. Orange color of the title compound were obtained from the mother solution on cooling [14].

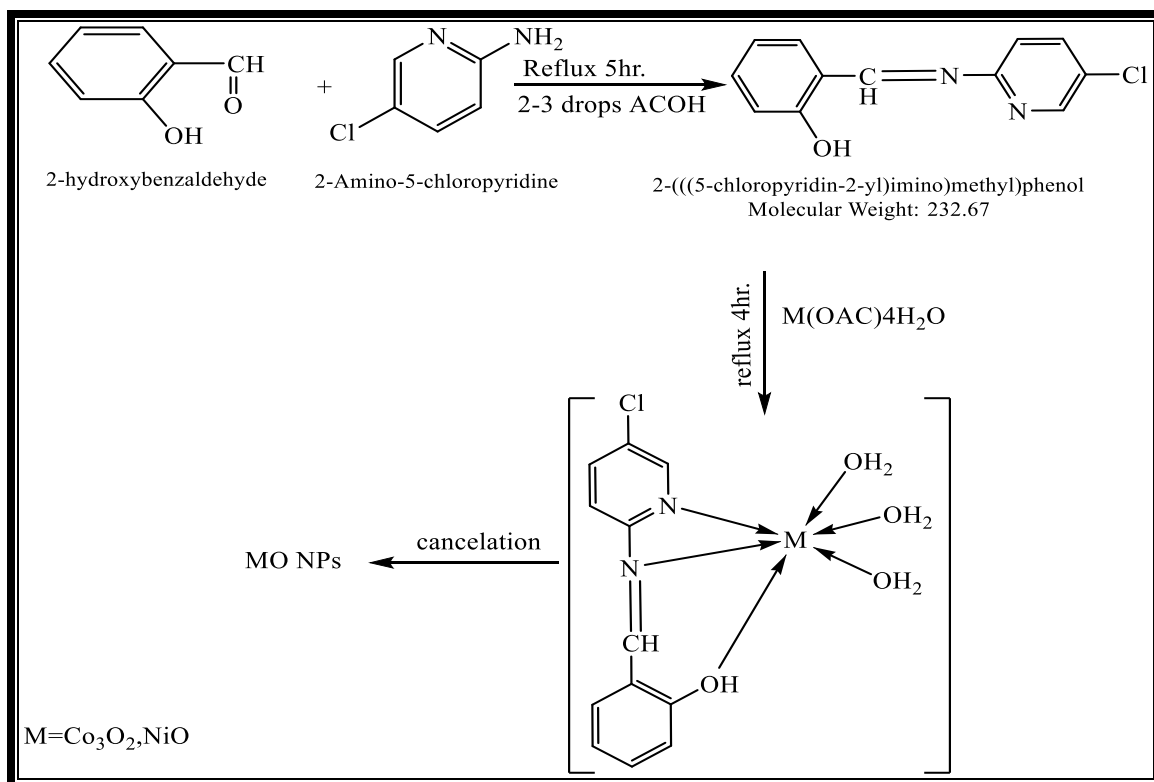
Synthesized metal ion complexes :

The synthesis of Zn(II) and Co(II) Schiff base complexes are shown in Scheme 1. About (1 gm, 0.004 mol of Schiff base (Ligand) in 25 mL ethanol was added to aqueous solution of cobalt(II) acetate (1.07 gm, 0.0004 mole) or Nickel (II)

acetate (1.69gm,0.004 mmol/25 mL) and heated under refluxed for four hours. After that, obtained solid product was filtered .

Synthesized of Co_3O_4 and NiO metal oxide nanoparticles

Thermal decomposition of the as-synthesized Co (II) and Ni (II) - Schiff base complexes for 4h at 550 oC in an electric furnace produced nano-sized Co_3O_4 and NiO, respectively[15, 16]



Scheme 1: Synthesis Schiff base (Ligand),metal ion complexes and metal oxides

Results and discussion :

FT-IR spectra of Ligand (Schiff base),Metal ion complexes and metal oxide nanoparticles

The FT-IR spectra (KBr pellets) are showed in Fig.1 and in Table 1 are listed. The positions of functional groups for the prepared ligand, complexes and metal oxide nanoparticles were showed strong stretching bands in the 1608 cm^{-1} region confirming the formation of azomethine linkage(s). The band at appearance of a 3150 cm^{-1} due to $\nu(\text{O-H})$ of the phenol group, proving the existence of a strong intramolecular hydrogen bonding [14, 15]. A slight shift in peak position was observed after complex formation. The shifting of bands corresponding to nitrogen atom of amine (azomethine) group, hydroxyl group of salicylaldehyde and (C=N) of pyridine ring indicates the coordination of metal to the ligand resulting formation of complexes [16]. Also, the band at approx. 1578 cm^{-1} which was assigned to the frequency of the C=N in the pyridine moiety was shifted slightly to lower frequencies in the spectra of the metal complexes. This shift suggests that the coordination takes place also through the pyridine ring nitrogen to the metal ion [16]. The FTIR spectrum of Co_3O_4 nanoparticles rendered significant absorption peaks at 580 and 670 cm^{-1} . The absorption band at 580 cm^{-1} was assigned to Co-O stretching vibration mode [17] and 661 cm^{-1} was assigned to the bridging vibration of O-Co-O bond [18]. The strong band at 490 cm^{-1} corresponds to the banding vibration of NiO. The band at 3445 cm^{-1} and the band in 1383 in Fig.(1) are due to the fact that the calcined powder tends to physically absorb water and carbonate ion [19].

Table (1) FT-IR spectra for Ligand, Metal ion complexes and Metal oxide nanoparticles

Compound	$\nu\text{C}=\text{N}$	$\nu(\text{C}=\text{N})$ ring	$\nu(\text{O-H})$	M-O	M-N
----------	------------------------	-------------------------------	-------------------	-----	-----

	cm ⁻¹	cm ⁻¹	cm ⁻¹	MOM cm ⁻¹	
Ligand (L)	1608	1570	3350	---	----
[Co(L)(H ₂ O) ₃]2CH ₃ COOH	1603	1560	3100	420	530
[Ni(L)(H ₂ O) ₃]2CH ₃ COOH	1620	1538	3270	420	570
Co ₃ O ₂ ,CoO	---	----	----	670	----
NiO	---	----	---	490	

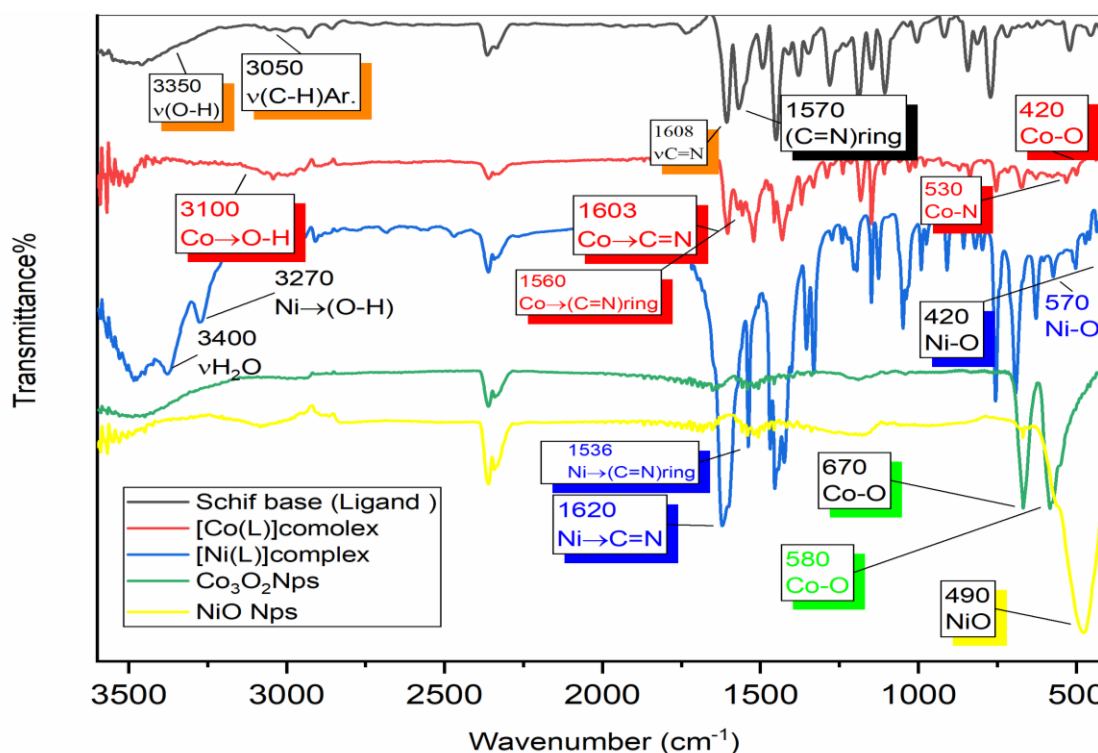


Figure 1: FTIR spectra for Schiff base (Ligand),metal ion complexes and metal oxides

Electronic spectra of for Ligand and its metal ion complexes :

Electronic spectra of Nickel (II) complex

The electronic spectrum of nickel (II) complex **Figure (2)** shows three bands at 8150, 14577.26 and 25000 cm⁻¹ which assigned to ³A_{2g}→³T_{2g}

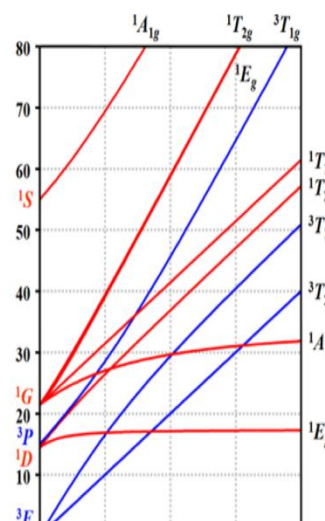


Figure2 Tanabe-Sugano diagram for the d⁸ electron configuration in the octahedral

, ${}^3A_{2g} \rightarrow {}^3T_{1g(F)}$ and ${}^3A_{2g} \rightarrow {}^3T_{1g(P)}$ transitions respectively. These bands indicate an octahedral geometry. The value for the first transition is approximately equal to calculated crystal field splitting energy, the value of the nephelauxetic factor β and Racah parameter B' were calculated by fitting the ratio ν_2/ν_1 to the Tanabe-Sugano diagram for octahedral d^8 system. The ratio $\nu_2/\nu_1 = 1.78$ fits the diagram at $1.1 Dq/B'$; therefore, from $E_2/B' = 22$ and $E_2/B' = 12.5$, B' will be 662.6 and $\beta = 0.63$ (taking B^0 of free ion to be 1035 cm^{-1}). This value confirms that the bond is covalency, the value of the constant field splitting $10Dq$ will be 8282.5 cm^{-1} , **Table (2)**. By fitting the ratio of frequencies (ν_2/ν_1) which equals to 1.74 indicates that the complex has a distorted octahedral geometry, while the value of a regular octahedral geometry equals to 1.6. [20-22]

Electronic spectra of cobalt (II) complex

The electronic spectrum of (LCo), figure 3-26, shows two spin-allowed bands in the visible region at (650nm, 15384.62 cm^{-1}) and (400nm, 25000 cm^{-1}), which might be assigned to the transition ${}^4T_{1g} \rightarrow {}^4A_{2g} (F) (\nu_3)$ and ${}^4T_{1g} \rightarrow {}^4T_{1g} (P) (\nu_2)$ respectively, the bands positions agree with the reported for an octahedral geometry [168]. Refer to the Tanabe-Sugano diagram, the numerous parameters of ligand field (ν_1 , B , β and Dq) have been calculated for d^7 configuration, Scheme 3-5, to be [(1205nm, 8296 cm^{-1}), 488, 0.502 and 8247.2] respectively. (β) factor of the nephelauxetic was calculated and found to be (0.502) representative bonding was a high degree of covalence from atoms in ligand donor with cobalt (II) ion [163], as well as the calculated value of (ν_1) to be (8296 cm^{-1}) due to the transition ${}^4T_{1g} \rightarrow {}^4T_{2g}$.

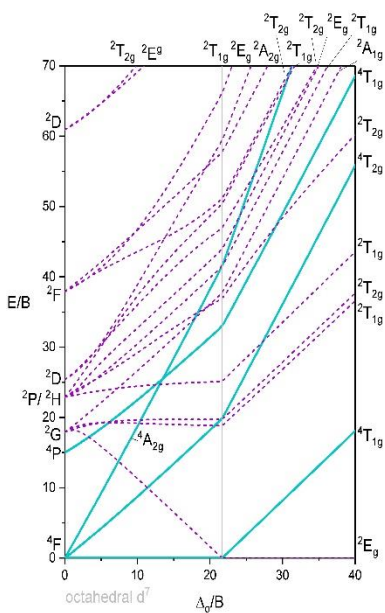


Figure 3 Tanabe-Sugano diagram for the d^7 electron configuration in the octahedral

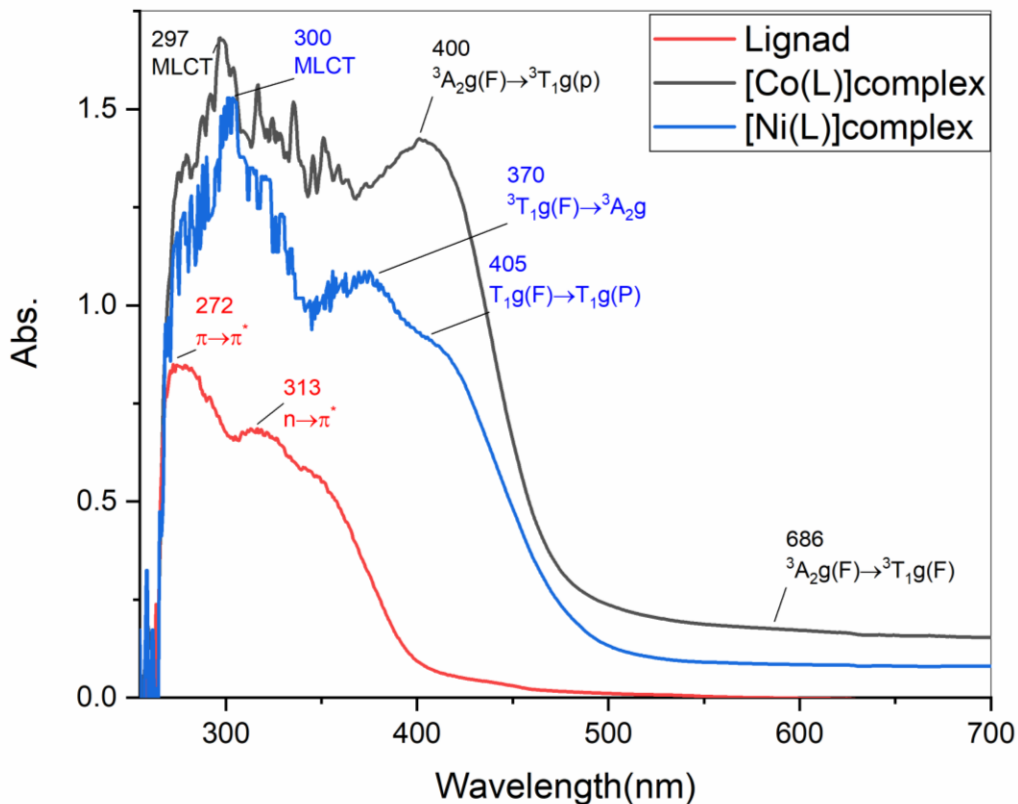


Figure 4 Electronic spectra for Schiff base (Ligand) and metal ion complexes

XRD for Metal oxide nanoparticles

The XRD pattern of calcination product (Fig. 5) indicates the simultaneous formation of Co_3O_4 nanoparticles. Bragg's reflections located at about 2θ values of 19.02, 31.30, 36.77, 38.58, 44.64, 55.77, 59.22 and 65.12 and 78.37° are attributed to the crystal planes of ((111), (220), (311), (222), (400), (422), (511), (440) and (622)), respectively. These planes are in agreement with the cubic phase Co_3O_4 (space group $\text{Fd}\bar{3}\text{m}$, JCPDS file no. 09-0418). The lattice constant calculated for the sample ($a = 0.8084 \text{ nm}$) is consistent with the standard value for Co_3O_4 ($a = 0.8065 \text{ nm}$). On the other hand, the five crystal planes of ((111), (200), (220), (311) and (222)) observed at about 2θ values of 36.87, 42.39, 61.49, 73.67. The crystallite size of Co_3O_4 nanoparticles, calculated by Scherrer equation 71 nm

The purity and crystallinity of the as-synthesized NiO nanoparticles were examined by using powder X-ray diffraction (XRD) as shown in Figure 1. It can be seen from Figure 1 that the diffraction peaks are low and broad due to the small size effect and incomplete inner structure of the particle. The peaks positions appearing at $2\theta = 37.20^\circ$, 43.20° , 62.87° , 75.20° , and 79.38° can be readily indexed as (111), (200), (220), (311), and (222) crystal planes of the bulk NiO, respectively. All these diffraction peaks can be perfectly indexed to the face-centered cubic (FCC) crystalline structure of NiO, not only in peak position, but also in their relative intensity of the characteristic peaks, which is in accordance with that of the standard spectrum (JCPDS, No. 04-0835). The XRD pattern shows that the samples are single phase and no any other impurities distinct diffraction peak except the characteristic peaks of FCC phase NiO was detected. This result shows that the physical phases of the NiO nanoparticles have higher purity prepared in this work. The NiO lattice constant calculated from the XRD data is 4.1729 Å, which is in good agreement with the reported data ° (JCPDS, No. 04-0835).

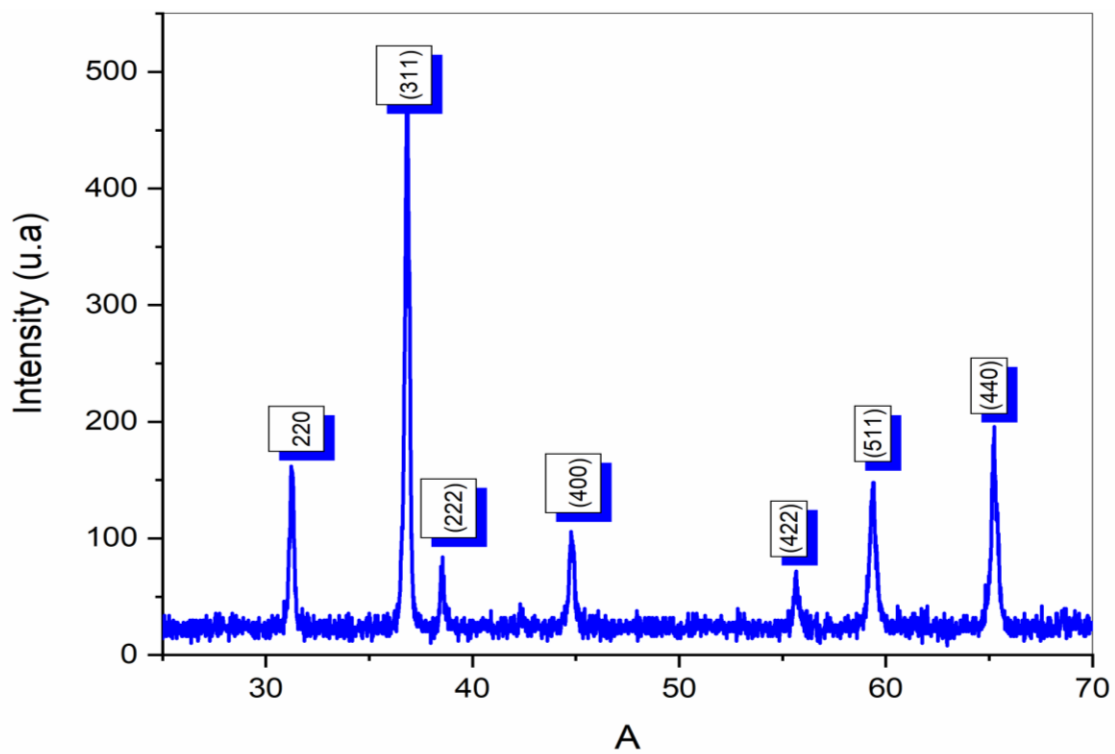


Figure6 XRD for cobalt oxide nanoparticles

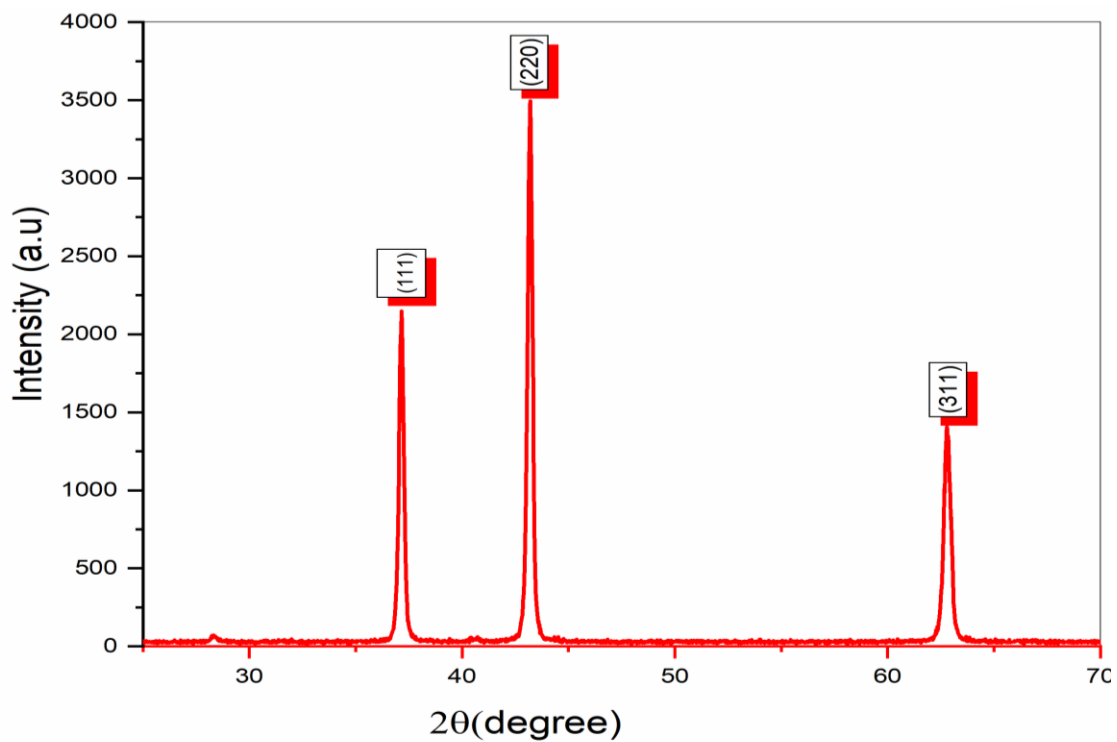


Figure8 XRD for Nickel oxide nanoparticles

conclusion

Salicylaldehyde, 2-Amino-5-chloropyridine, and Metal acetate were used to create a binary Metal ion Schiff-base complex. FTIR, $^1\text{H-NMR}$, $^{13}\text{C-NMR}$, and UV-Vis were utilized to determine the structure of the new M(II) complex produced and describe the formation of Schiff base ligand and metal with a molar ratio of 1:1. These observations led to the suggestion of deformed octahedral molecular for the Ni and Co(II) complexes. Adopting the self-prepared [M (L)] as the precursor, Co_3O_4 and NiO nanoparticles have been synthesized by the thermal treatment method. By thermal decomposition of Ni(II) and Cu(II) Schiff base complex, NiO and CuO nanoparticles that confirmed by XRD with average particle size about 23.8nm and 22.9 nm respectively are uniformly formed in polycrystalline monoclinic and cubic structures, respectively, without any observed impurity phases.

References

1. Parsaee, Z., K. Mohammadi, M. Ghahramaninezhad, and B.J.N.J.o.C. Hosseinzadeh, *A novel nano-sized binuclear nickel (II) Schiff base complex as a precursor for NiO nanoparticles: synthesis, characterization, DFT study and antibacterial activity*. 2016. **40**(12): p. 10569-10583.
2. Devi, J., N. Batra, R.J.S.A.P.A.M. Malhotra, and B. Spectroscopy, *Ligational behavior of Schiff bases towards transition metal ion and metalation effect on their antibacterial activity*. 2012. **97**: p. 397-405.
3. Singh, A., H.P. Gogoi, and P.J.I.C.A. Barman, *Synthesis of metal oxide nanoparticles by facile thermal decomposition of new Co (II), Ni (II), and Zn (II) Schiff base complexes-optical properties and photocatalytic degradation of methylene blue dye*. 2023. **546**: p. 121292.
4. Barakat, M., R. Kumar, T. Almeelbi, B.A. Al-Mur, and J.O.J.J.o.C.P. Eniola, *Sustainable visible light photocatalytic scavenging of the noxious organic pollutant using recyclable and reusable polyaniline coupled WO₃/WS₂ nanohybrid*. 2022. **330**: p. 129942.
5. Abdel-Rahman, L.H., A.M. Abu-Dief, R.M. El-Khatib, and S.M.J.B.c. Abdel-Fatah, *Some new nano-sized Fe (II), Cd (II) and Zn (II) Schiff base complexes as precursor for metal oxides: Sonochemical synthesis, characterization, DNA interaction, in vitro antimicrobial and anticancer activities*. 2016. **69**: p. 140-152.
6. Nassar, M.Y., A.S. Attia, K.A. Alfallous, and M.J.I.C.A. El-Shahat, *Synthesis of two novel dinuclear molybdenum (0) complexes of quinoxaline-2, 3-dione: new precursors for preparation of α -MoO₃ nanoplates*. 2013. **405**: p. 362-367.

7. Nassar, M., T. Mohamed, and I.J.J.o.M.S. Ahmed, *One-pot solvothermal synthesis of novel cobalt salicylaldehyde–urea complexes: a new approach to Co₃O₄ nanoparticles*. 2013. **1050**: p. 81-87.
8. Aly, H.M., M.E. Moustafa, M.Y. Nassar, and E.A.J.J.o.M.S. Abdelrahman, *Synthesis and characterization of novel Cu (II) complexes with 3-substituted-4-amino-5-mercapto-1, 2, 4-triazole Schiff bases: a new route to CuO nanoparticles*. 2015. **1086**: p. 223-231.
9. Davar, F., M. Salavati-Niasari, N. Mir, K. Saberyan, M. Monemzadeh, and E.J.P. Ahmadi, *Thermal decomposition route for synthesis of Mn₃O₄ nanoparticles in presence of a novel precursor*. 2010. **29**(7): p. 1747-1753.
10. Jia, W., E. Reitz, P. Shimpi, E.G. Rodriguez, P.-X. Gao, and Y.J.M.R.B. Lei, *Spherical CuO synthesized by a simple hydrothermal reaction: concentration-dependent size and its electrocatalytic application*. 2009. **44**(8): p. 1681-1686.
11. Singh, A.K.J.C.R.i.G. and S. Chemistry, *A review on plant extract-based route for synthesis of cobalt nanoparticles: Photocatalytic, electrochemical sensing and antibacterial applications*. 2022: p. 100270.
12. Al Zoubi, W., M.P. Kamil, S. Fatimah, N. Nashrah, and Y.G.J.P.i.M.S. Ko, *Recent advances in hybrid organic-inorganic materials with spatial architecture for state-of-the-art applications*. 2020. **112**: p. 100663.
13. Al Zoubi, W., N. Nashrah, R. Putri, A. Allaf, B. Assfour, and Y.J.M.T.N. Ko, *Strong dual-metal-support interactions induced by low-temperature plasma phenomenon*. 2022. **18**: p. 100213.
14. Silverstein, R.M. and G.C.J.J.o.C.E. Bassler, *Spectrometric identification of organic compounds*. 1962. **39**(11): p. 546.

15. Subhi, H.M., A.T. Bader, and H.Y.J.I.J.o.C. Al-Gubury, *Synthesis and Characterization of ZnO Nanoparticles via Thermal Decomposition for Zn (II) Schiff Base Complex*. 2022.
16. Jeewoth, T., H. Li Kam Wah, M.G. Bhowon, D. Ghoorohoo, K.J.S. Babooram, R.i. Inorganic, and M.-O. Chemistry, *Synthesis and anti-bacterial/catalytic properties of Schiff bases and Schiff base metal complexes derived from 2, 3-diaminopyridine*. 2000. **30**(6): p. 1023-1038.
17. Estepa, L. and M.J.B. Daudon, *Contribution of Fourier transform infrared spectroscopy to the identification of urinary stones and kidney crystal deposits*. 1997. **3**(5): p. 347-369.
18. Wu, S.-H., D.-H.J.J.o.C. Chen, and I. Science, *Synthesis and characterization of nickel nanoparticles by hydrazine reduction in ethylene glycol*. 2003. **259**(2): p. 282-286.
19. Bahari Molla Mahaleh, Y., S. Sadrnezhad, and D.J.J.o.N. Hosseini, *NiO nanoparticles synthesis by chemical precipitation and effect of applied surfactant on distribution of particle size*. 2008. **2008**: p. 1-4.
20. Gopalan, R., *Concise coordination chemistry*. 2001: Vikas publishing house.
21. Figgis, B.N. and M.A. Hitchman, *Ligand field theory and its applications*. 1999.
22. Reshma, R., R. Selwin Joseyphus, D. Arish, R.J. Reshmi Jaya, J.J.J.o.B.S. Johnson, and Dynamics, *Tridentate imidazole-based Schiff base metal complexes: Molecular docking, structural and biological studies*. 2022. **40**(18): p. 8602-8614.